

Fundamental Issues in Fast Ignition Physics: from Relativistic Electron Generation to Proton Driven Ignition

A. Macchi 1), A. Antonicci 2), S. Atzeni 3), D. Batani 4), F. Califano 1), F. Cornolti 1), J. J. Honrubia 2), T. V. Lisseikina 1), F. Pegoraro 1), M. Temporal 5)

1) Istituto Nazionale per la Fisica della Materia (INFN), sezione A, Dipartimento di Fisica, Università di Pisa, Italy

2) ETSII, Universidad Politecnica de Madrid, Spain

3) Dipartimento di Energetica, Università di Roma “La Sapienza” and INFN, Roma, Italy

4) Dipartimento di Fisica, Università di Milano “Bicocca” and INFN, Milano, Italy

5) ETSII, Universidad de Castilla-La Mancha, Spain

e-mail contact of main author: macchi@df.unipi.it

Abstract. In recent years, several schemes for laser-driven Fast Ignition (FI) of Inertial Confinement Fusion (ICF) targets have been proposed. In all schemes, a key element is the conversion of the energy of a Petawatt laser pulse into a beam of strongly relativistic electrons and the transport of the latter into a dense plasma or a solid target. The electron beam may either drive ignition directly or be used to accelerate a proton beam which is in turn used to ignite. Both ignition scenarios involve a number of physical processes which are widely unexplored and challenging for theory and simulation. In this contribution, we present theoretical and numerical investigations of several fundamental issues of relevance to FI from the stage of electron generation and transport to that of proton energy deposition, including electron beam instabilities, transport in solid-density materials, and requirements for proton beam driven ignition.

1. Introduction

An essential element of Fast Ignition (FI) of ICF targets is the conversion of the energy of a Petawatt laser pulse into a beam of strongly relativistic electrons. In the original proposal [1], the electron beam is generated by direct interaction of the laser pulse with the coronal plasma and reaches the precompressed fuel core after propagating in the dense plasma region. The electron beam is expected to carry a current of several MegaAmperes, and its transport properties are thus affected by self-generation of very high electric and magnetic fields, beam instabilities, and inefficient charge neutralization due to low conductivity of background electrons. Efficiency of energy transport is also a key factor in alternative FI schemes [2]. Electric field generation by relativistic electrons penetrating in solid targets is also important as an accelerating mechanism of hydrogen ions (i.e. protons), which may be present in the target material either as a component or an impurity. The proton beam may be intense enough to provide an alternative driver for FI, as suggested in a more recent proposal [3].

On the route from fast electron generation to ignition, many physical processes are at play and the resulting scenario is therefore quite complex. One needs, for example, to understand the basic physics of processes such as generation of electron jets and related beam instabilities, or to develop simulation models to support test-bed experiments. The final goal is, of course, to estimate the energy of the driving laser pulse for a given ignition scheme. This requires to collect and integrate the information provided by basic theory, experiments and simulation as much as possible. In this paper, we present several

investigations of physical processes relevant to FI which have been performed within our collaboration project.

2. Fast electron filaments: Weibel or surface instabilities ?

The basic process of relativistic (or “fast”) electron generation by high-intensity laser interaction with an overdense plasma is mostly studied with particle-in-cell (PIC) simulations. Many of such simulation studies have evidenced a filamentary structure of the fast electron current penetrating into the plasma, with filaments originating immediately after the laser-plasma interaction region either in 2D [4,5] and 3D [6] geometry. The origin of current filaments has been often attributed to a beam instability of the Weibel type, driven by the magnetic repulsion between the fast electron current and the oppositely directed “return” current of “cold” background electrons.

Motivated by the role attributed to the Weibel instability in the electron transport process, we have analyzed its nonlinear regime in 3D by performing relativistic, collisionless fluid simulations. The simulations are initialized assuming two oppositely directed electron beams with zero net current, i.e. $n_1 v_1 = -n_2 v_2$ where $n_{1,2}$ and $v_{1,2}$ are the beam densities and velocities, respectively, and $n_1 + n_2 = n_0$ where n_0 is the total electron density. A highly asymmetrical configuration ($n_1/n_2 = 9$, $v_1 = 0.95c$, $v_2 = -0.10556c$) was simulated. This corresponds to fast electrons with 1 MeV energy carrying, for $n_0 = 10^{28} \text{ m}^{-3}$ (typical of PIC simulations), an energy flux equal to $4.6 \times 10^{22} \text{ W m}^{-2}$. A white random noise of amplitude $\simeq 10^{-6}$ times the initial values is added as a seed for the instability. The dimensions of the numerical grid were $64 \times 64 \times 128$ with a spatial resolution of $\simeq 0.5d_e$, where $d_e = c/\omega_p$ is the electron skin depth and $\omega_p = \sqrt{n_0 e^2 / \epsilon_0 m_e}$ is the plasma frequency.

In Fig.1 the component of the vector potential along the beam direction (A_z) at $t = 60\omega_p^{-1} \simeq 10 \text{ fs}$ for $n_0 = 10^{28} \text{ m}^{-3}$ is shown. It is convenient to show A_z because the magnetic field generated by the instability lies predominantly in the plane perpendicular to the beams, i.e. $B_z \ll B_x, B_y$. We thus see that the development of the Weibel instability in 3D generates magnetic structures with typical length scales comparable to a few times d_e both in the direction of the beams and in the perpendicular plane, in contrast to what is generally observed in PIC simulations where the filaments extend along the beam direction for hundreds of d_e . Furthermore, as observed also at later times before entering the nonlinear regime, there is no inverse cascade in the (x, y) plane (as well as in the (x, z) and (y, z) planes), in contradiction with the results obtained in purely 2D simulations in the plane perpendicular to the beam direction, as for example in [7]. This last result is not surprising since inverse cascade processes are typical of 2D systems.

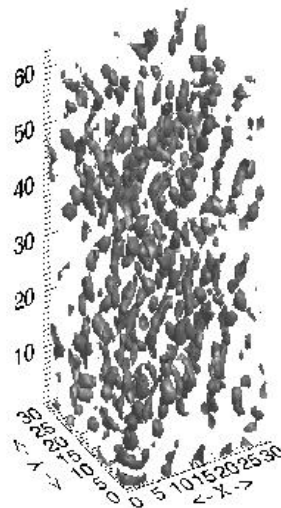


FIG.1. 3D Fluid simulation of the Weibel instability: isocontours of A_z at $t = 60\omega_p^{-1}$. Axis labels are in units of d_e . See text for parameters.

These numerical results are consistent with the observation that in this parameter range, the wave vector of the most unstable mode is not strictly perpendicular to the beam direction. In particular, by solving numerically the full dispersion relation [8] for the

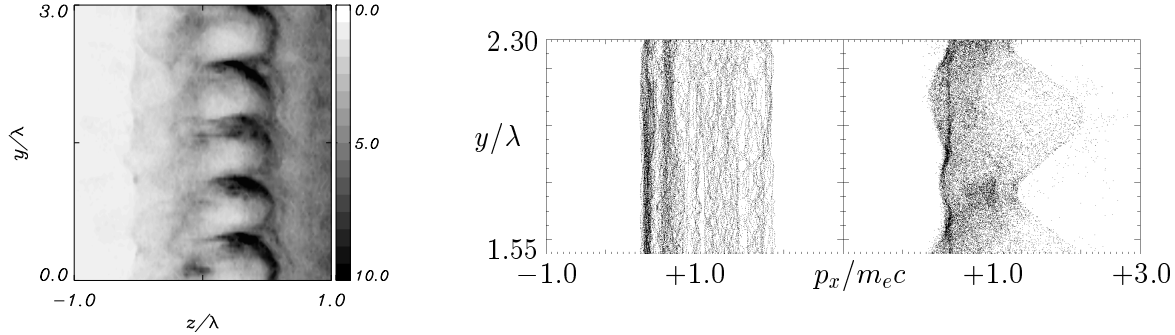


FIG.2. 2D PIC simulations of the interaction of a 10^{23} W/m², laser pulse with an overdense plasma. Left: density contours showing the onset of surface ripples due to parametric instabilities. Right: phase space projections showing longitudinal electron acceleration correlated with ripple locations.

simulation parameters, the maximum growth rate is found at $k_{\parallel} \simeq 0.8$ and $k_{\perp} \geq 2.0$. Furthermore, the growth rate curve becomes nearly flat for smaller values of k_{\parallel} in the range $0 \leq k_{\parallel} \leq 0.5$ and decreases very rapidly for larger values of $k_{\parallel} > 1$. These results are quite typical of the relativistic case and do not depend qualitatively on the particular parameter choice [8]. For the parameters of the simulation reported, the analytical maximum growth rate is $\gamma_{th} \simeq 0.2\omega_p$, close to the value observed in simulations $\gamma_{num} = 0.18\omega_p$.

An alternative picture for the generation of fast electron filaments has been recently discussed on the basis of 2D PIC simulations which showed the generation of a standing, “period-doubling” oscillation at the plasma surface due to the onset of laser-stimulated parametric instabilities [9]. In the low-intensity regime the process is understood as the parametric excitation of counterpropagating surface waves [10]. Fig.2 shows results for a laser pulse of intensity 10^{23} W/m² and wavelength $0.25 \mu\text{m}$ impinging on a step-boundary plasma with initial density 8×10^{26} m⁻³. Phase space projections before and after the growth of surface instabilities show that fast electrons are accelerated mostly near the maxima of the standing surface oscillations, leading to an “imprint” for a filamentary structure. This apparent relation between fast electron jets and surface instabilities is attractive since it would imply that the filaments are generated already at the plasma surface (i.e. over a very narrow region, in contrast to the “Weibel” picture which assumes an initial state of nearly homogeneous currents), that their location is correlated with that of density “ripples” at the plasma surface, and (at least when the dispersion relation of surface modes resembles that of linear surface waves) that their transverse dimensions scale approximately with the laser wavelength. All these features have been observed in several simulations.

3. Modeling electron transport in solid targets

The study of fast electron transport in solid targets provides a test bed for the stage of energy transport into the core. The penetration of fast electrons is mainly diagnosed by K- α emission. The importance of self-generated electric fields was evidenced by comparing results for different type of materials, e.g. metallic and dielectric targets [11]. In fact, in a low-conductivity material (e.g., a dielectric target) the return current of cold background electrons may be strongly quenched, resulting in strong back-holding electric fields.

The use of foam targets, having a controllable average density which is less than that of a solid target, was effective in giving a further evidence of electric field inhibition [12]. As was done in previous experiments [11] the targets had the same Al coating on the front side, to ensure that the fast electron source was the same for all targets. On the rear side the targets were coated with fluor materials to produce K- α emission. For purely collisional transport the penetration depth R and the K- α yield would be proportional to $(\rho)^{-1}$ and to ρL , respectively, where ρ and L are the target density and thickness. Fig.3 shows the K- α yield from both two fluor materials (Mo,Pd), plotted against areal density from foams and normal density plastics. As we can see there is an approximate power law scaling with a slope 0.52 for both Pd and Mo. Since the areal density ρL is the same for all targets, the reduction of K- α yield when target density is decreased gives a further evidence of inhibition of fast electron penetration by self-generated fields.

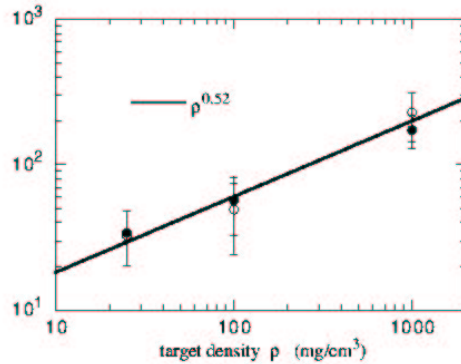


FIG.3. K- α yield from foam plastic targets with constant mass thickness ρL .

To develop an improved tool to analyse fast electron transport experiments, the 3D MC electron-photon transport code PENELOPE [13] has been adapted by including electron injection, field generation and diagnostics [14]. The field generation model is analogous to that of similar hybrid codes [15, 16]. The code has been used to simulate the experiments of Ref. [11]. A total energy of 5 J delivered in 350 fs (fwhm) into a focal spot diameter of 10 μm , which corresponds to a laser intensity of $1.8 \times 10^{23} \text{ W/m}^2$, and a conversion efficiency of 25% were assumed. Electrons propagated through a transport layer of Al or CH, followed by two fluor layers of Mo and Pd. The results for K- α yield are shown in Fig.4. The mean energy of electrons comes out from fitting the numerical results to the experimental points. For Al targets, the calculations performed with fields not included or included, give a value for the mean energy of 500 keV and 560 keV, respectively. Thus, the effect of self-generated fields is significant even in conducting materials. In the case of plastic targets, electric inhibition is greater as consequence of its high resistivity at low temperatures. The resistivity of plastic has been taken from the heuristic model of Ref. [15].

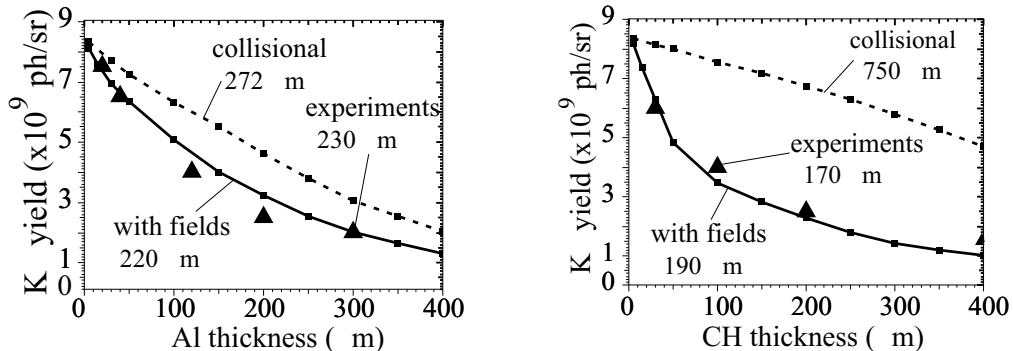


FIG.4. Simulations of fast electron transport in solid targets with the hybrid MC-fluid code derived from the PENELOPE code: experimental and calculated K- α yield vs. thickness for Al (left) and plastic targets (right).

The pinching effect of self-generated magnetic fields on the fast electron beam can be seen by comparing the time-integrated K- α distribution in the azimuthal plane (integrated in time and in the direction of propagation) with and without fields, shown in Fig.5 for the Al target of $50\mu\text{m}$. If fields are not taken into account, electrons propagate with a cone angle of 30 degrees (i.e., diameter of beam at the fluor layer of, roughly, $60\mu\text{m}$). When fields are turned on, the collimation of the electron beam is enhanced. In this simulation, the energy balance is as follows: 26% of the fast electron energy is transferred to the plasma by joule heating due to the return current, 23% deposited by collisions of fast electrons and the remainder is leaked out. In the case of the plastic target, 54% of the energy goes into joule heating and 15% into collisions. Thus, self-generated fields are important in both cases, but play a prominent role in non-conducting materials, as expected.

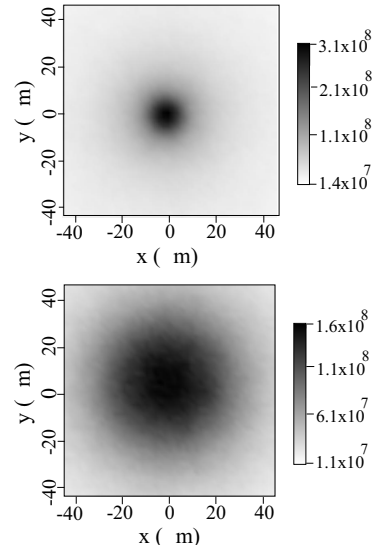


FIG.5. PENELOPE simulations: K- α distribution in the azimuthal plane for Al targets with fields turned on (top) and off (bottom).

The assumption of local charge quasi-neutrality, neglecting electrostatic fields (i.e. the electric field is purely inductive) [14–16] is reasonable for a good conductor, but is more questionable for low conductivity materials. For this reason an hybrid transport code which includes electrostatic effects is under development. Here we report preliminary results in a 1D geometry, which implies that the electrostatic field is overestimated; however, results are indicative at least as far as the penetration distance of fast electrons is less than the laser spot radius. In Fig.6, simulation results for the propagation of 200 keV electrons into an Al isothermal plasma with a temperature of 100 eV are shown at the time $t = 100$ fs from the simulation start. The flux of fast electrons is constant in time (“flat-top” pulse) and corresponds to an intensity of 3.6×10^{21} W/m². Both the field profiles and the phase space distributions evolve slowly and look very similar at following times, as far as the injected fast electron current is constant. It is found that most of the fast electrons injected into the plasma are kept near the surface by a capacitor-like electrostatic field within a few microns at the time shown ($t = 100$ fs), and only a small fraction propagates deeper into the target. The electrostatic field is mostly generated by surface charges, while charge neutralization is very well satisfied in the plasma volume.

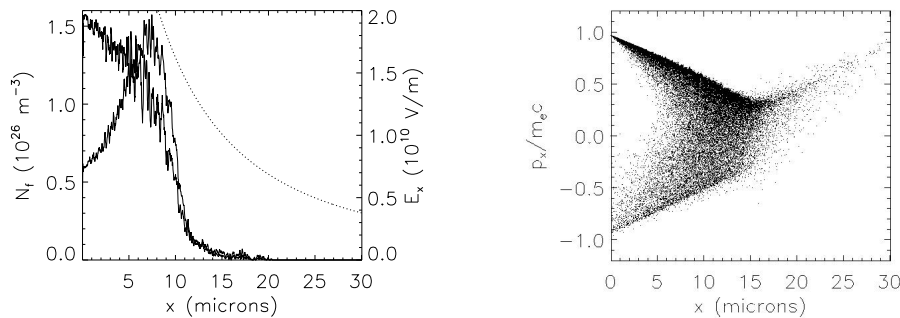


FIG.6. 1D Simulations of electrostatic stopping of a 200 keV, 3.6×10^{21} W/m² fast electron beam injected into an Al plasma with a 200 eV temperature. Left: profiles of fast electron density (thin line), electric field (thick), and analytical predictions of Ref. [17] (dotted). Right: $(x - p_x)$ phase space of fast electrons. Broadening in momentum space is due to Coulomb collisions.

In Fig.6 the fast electron density profile is compared with the analytical solution given in Ref. [17] for an homogeneous, isothermal plasma with efficient charge neutralization. The analytical modeling of Ref. [17] assumes that the fast electron distribution is confined by the electrostatic field and the density profile is normalized to the total number of electrons injected into the target. The numerical results are very different from the analytical predictions. One reason for this discrepancy is that most of the injected electrons are actually reflected from the surface field and go back to the surface, so the total number of electrons inside the target is much smaller than the total number of electrons injected at that time.

4. Requirements for proton beam driven ignition

A few years ago, beam requirements for fast ignition had been evaluated assuming that the hot spot is created by pulses of particles with assigned range and constant stopping power [18]. For optimally focused pulses, the minimum beam energy and power required to ignite a DT sphere with density ρ are, respectively $E_{\text{opt}} = 140/\hat{\rho}^{1.85}$ kJ, and $P_{\text{opt}} = 2.6/\hat{\rho}$ PW, where $\hat{\rho} = \rho/[10^5 \text{ kg/m}^3]$. The optimal focal radius is $r_{\text{opt}} \approx 60/\hat{\rho}$ μm . The recent proposal of fast ignition by laser accelerated proton beams [3] has motivated new studies, because i) laser-induced proton sources have wide energy spectra; ii) the associated velocity dispersion may give rise to substantial power spread at the dense fuel, located at distance d from the source; iii) proton stopping power in a dense target can be described by accurate models, including the dependence on proton energy and plasma density and temperature.

Proton beam requirements for DT fast ignition have then been studied by an analytical model and by 2D numerical radiation-hydro-nuclear simulations integrated with 1D simulations of fuel compression [19, 20]. The simulations assume that the beam is optimally focused and the proton velocity distribution is exponential or maxwellian. We have first considered the ignition of homogeneously precompressed DT spheres, and have determined the proton energy required as a function of fuel density, proton beam temperature T_p and source-to-fuel distance d . Results for fuel density $\rho = 4 \times 10^5 \text{ kg/m}^3$ are shown in Fig. 7. Simulations for different densities show that the optimal T_p is in any case about 5 MeV. For $d = 1 - 4$ mm and optimal T_p , the ignition energy is reasonably fitted by $E_{ig}^* = 90(d/1 \text{ mm})^{0.7}/\hat{\rho}^{1.3}$ kJ. A simple analytical model [19] shows similar trends and helps in acquiring insight into the relevant physics. An important result is that the values of E_{ig}^* for $d = 3$ mm are higher by a factor about 4 than those estimated in earlier work [3]. Notice that the scaling of E_{ig}^* with density is weaker than found in Ref. [18]. Analogous results are found for fuel configurations generated by capsule implosion [20]. It is interesting to observe, however, that despite the larger than expected requirements for ignition, a target based on standard indirect drive implosion followed by proton driven ignition is estimated to achieve an energy gain of about 200 at a driver energy of about 2.5 MJ.

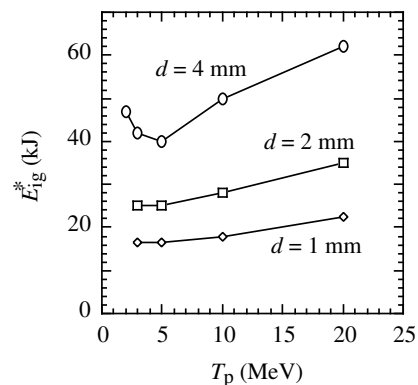


FIG.7. Minimum proton beam energy E_{ig}^* for ignition of a DT sphere ($\rho = 4 \times 10^5 \text{ kg/m}^3$, radius $R = 100 \mu\text{m}$) vs. average proton energy T_p and source-fuel distance d .

Frames of a 2D simulation of the ignition of a capsule with 3.5 mg of DT fuel, imploded after absorbing 635 kJ of 210 eV X-rays, are shown in Fig. 8. The simulations also show rather complex features related to the time-dependence of both the proton beam spectrum at the target, the fuel temperature and to the density spatial profile [20]. It is found that only a portion of the proton spectrum actually contributes to the generation of the ignition hot spot. By appropriately shaping the proton spectrum, the ignition energy could then be lowered by a factor larger than 2. Beam parameters can be made less demanding by placing the source very close to the fuel, as foreseen, e.g. by conical targets [21]. To understand relevant issues, we have performed a preliminary set of simulations, concerning the ignition of a sector of capsule, induced by a proton beam generated at very small distance from the sphere centre (e.g. $d = 0.5$ mm) [20]. These simulations confirm the substantial decrease of the required ignition energy ($E_{ig} = 12$ kJ for the case in the figure), without burn degradation. The feasibility of high-convergence implosion of sphere sectors thus becomes a key, and so far unexplored issue.

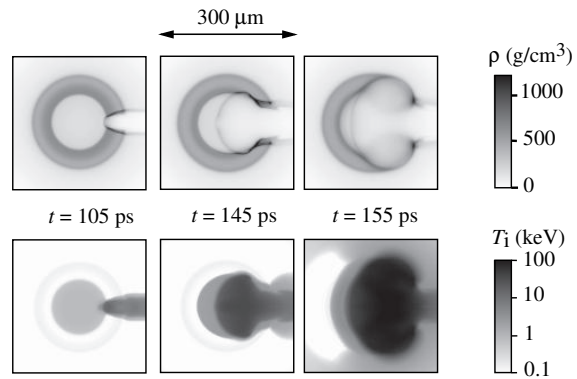


FIG. 8. 2D simulations of proton beam driven ignition of radiatively imploded fuels: ignition of a compressed spherical capsule heated by 26 kJ of protons released at $d = 4$ mm from the fuel.

Acknowledgments

This work was supported partly by the Istituto Nazionale per la Fisica della Materia (INFN) through the PAIS project GenTE and the Supercomputing Initiative, and by the Italian Ministry of University and Research (MURST-MIUR) through the project “Generazione di fasci di elettroni e ioni ...”. S.A. gratefully acknowledges two travel grants by the European Science Foundation FEMTO programme.

References

- [1] TABAK, M. et al., “Ignition and high gain with ultrapowerful lasers”, *Phys. Plasmas* **1** (1994) 1626.
- [2] HAIN, S., MULSER, P., “Fast ignition without hole boring”, *Phys. Rev. Lett.* **86** (2001) 1015.
- [3] ROTH, M., et al., “Fast ignition by intense laser-accelerated proton beams”, *Phys. Rev. Lett.* **86** (2001) 436.
- [4] LASINSKI, B., et al., “Particle-in-cell simulations of ultra intense laser pulses propagating through overdense plasma for fast-ignitor and radiography applications”, *Phys. Plasmas* **6** (1999) 2041.
- [5] SENTOKU, Y., et al., “Magnetic instability by the relativistic laser pulses in overdense plasmas”, *Phys. Plasmas* **7** (2000) 689.
- [6] SENTOKU, Y., et al., “Three-dimensional particle-in-cell simulations of energetic electron generation and transport with relativistic laser pulses in overdense plasmas”, *Phys. Rev. E* **65** (2002) 046408.

- [7] HONDA, M., et al., “Two-dimensional particle-in-cell simulation for magnetized transport of ultra-high relativistic currents in plasma”, *Phys. Plasmas* **7** (2000) 1302.
- [8] CALIFANO, F., et al., “Nonlinear filamentation instability driven by an inhomogeneous current in a collisionless plasma”, *Phys. Rev. E* **58** (1998) 7837.
- [9] MACCHI, A., et al., “Surface oscillations in overdense plasmas irradiated by ultra-short laser pulses”, *Phys. Rev. Lett.* **87** (2001) 205004.
- [10] MACCHI, A., et al., “Two surface-wave decay”, *Phys. Plasmas* **9** (2002) 1704.
- [11] PISANI, F., et al., “Experimental evidence of electric inhibition in fast electron penetration and of electric-field-limited fast electron transport in dense matter”, *Phys. Rev. E* **62** (2000) R5927.
- [12] BATANI, D., et al., “Inhibition in the propagation of fast electrons in plastic foams by resistive electric fields”, *Phys. Rev. E* **65** (2002) 066409.
- [13] BARÓ, J., et al., “PENELOPE: An algorithm for Monte Carlo simulation of the penetration and energy loss of electrons and positrons in matter”, *Nucl. Instr. Meth. Phys. Research B* **100** (1995) 31.
- [14] ANTONICCI, A., et al., “Development of a simulation model for fast electron transport in solid and plasmas”, *EPS Conference on Controlled Fusion and Plasma Physics - 5th Workshop on Fast Ignition of Fusion Targets (Proc. 28th ESP Conf. - Funchal, Portugal, 2001)*, *Europhysics Conference Abstracts* **25A** (2001) 1.
- [15] DAVIES, J.R., “How wrong is collisional Monte Carlo modeling of fast electron transport in high-intensity laser-solid interactions?”, *Phys. Rev. E* **65** (2002) 026407.
- [16] GREMILLET, L., et al., “Filamented transport of laser-generated relativistic electrons penetrating a solid target”, *Phys. Plasmas* **9** (2002) 941.
- [17] BELL, A. R., et al., “Fast electron transport in high intensity short pulse laser-solid experiments”, *Plasma Phys. Contr. Fusion* **39** (1997) 653.
- [18] ATZENI, S., “Inertial fusion fast ignitor: Igniting pulse parameter window vs the penetration depth of the heating particles and the density of the precompressed fuel”, *Phys. Plasmas* **6** (1999) 3316.
- [19] ATZENI, S., et al., “A first analysis of fast ignition of precompressed ICF fuel by laser-accelerated protons”, *Nucl. Fusion* **42** (2002) L1.
- [20] TEMPORAL, M., et al., “Numerical study of fast ignition of ablatively imploded DT fusion capsule by laser-generated proton beams”, *Phys. Plasmas* **9** (2002) 3098.
- [21] KODAMA, R., et al., “Fast heating of ultrahigh-density plasma as a step towards laser fusion ignition”, *Nature* **412** (2001) 798.